

Large Language Model Enabled Multi-Task Physical Layer Network

Tianyue Zheng, *Student Member, IEEE*, and Linglong Dai, *Fellow, IEEE*

Abstract—The recent advance of Artificial Intelligence (AI) is continuously reshaping the future 6G wireless communications. Recently, the development of Large Language Models (LLMs) offers a promising approach to effectively improve the performance and generalization for different physical layer tasks. However, most existing works finetune dedicated LLM networks for a single wireless communication task separately. Thus performing diverse physical layer tasks introduces extremely high training resources, memory usage, and deployment costs. To solve the problem, we propose a LLM-enabled multi-task physical layer network to unify multiple tasks with a single LLM. Specifically, we first propose a multi-task LLM framework, which finetunes LLM to perform multi-user precoding, signal detection and channel prediction simultaneously. Besides, multi-task instruction module, input encoders, as well as output decoders, are elaborately designed to distinguish multiple tasks and adapted the features of different formats of wireless data for the features of LLM. Numerical simulations are also displayed to verify the effectiveness of the proposed method.

Index Terms—large language models (LLMs), multi-task LLM, physical layer communications

I. INTRODUCTION

The deep integration of Artificial Intelligence (AI) with wireless communications is one of the key features of Sixth-Generation (6G) communications [1]. With the development of 6G communications, the application of AI becomes important and essential to manage increasing complexity and user demands, and thereby supports more intelligent services and applications. In physical layer communications, owing to strong learning ability from data, AI especially deep learning (DL), has gained significant attention [2] and demonstrated great potential in a wide range of tasks, including CSI feedback [3], channel estimation [4] and prediction [5], signal detection [6], etc. Moreover, significant efforts have been made by 3rd Generation Partnership Project (3GPP) to standardize DL in wireless networks recently [7].

Despite the significant progress, existing DL empowered methods still face some fundamental issues limiting their application in practical scenarios. First, the capability of DL is constrained by the size of networks. With the increasingly high-dimension channel, complex network and rapidly changing environments, existing methods struggle to accurately

model the problem and capture features from a global perspective. Secondly, the deep learning-based methods are often sensitive to different wireless environments, and result in poor robustness and generalization, requiring retraining when the channel distribution changes. Recently, Large language models (LLMs) [8]–[10] have revolutionized AI domains and attracted considerable interest from both academia and industry, which offer an entirely new paradigm for solving the challenges of existing DL methods. Unlike previous DL algorithms, these models with a huge amount of parameters, possess the ability to capture universal knowledge and demonstrate impressive language understanding and generation capabilities to various tasks in different domains.

Therefore, explosive attention has explored the potential transformative impact of LLMs on wireless communications [11]–[15]. Moreover, a few works have focused on opening up new possibilities for improving the performance of different applications in physical layer communications. The authors in [16] propose a LLM-empowered channel prediction method to achieve improved predictive capability and generalization ability. [17] also unleashes the strength of LLMs for time series forecasting to improve the robustness of beam prediction. Besides, in [18] LLM is adopted to perform resource allocation by a few-shot learning-based approach, where the channel gains and the corresponding transmit power strategies are provided as references in the prompt of LLM, confirming the applicability and feasibility of LLM. However, most existing works finetune dedicated LLM networks for a *single* wireless communication task. Given the parameter size of LLM, designing and training dedicated models for each task separately leads to extremely high computational complexity, memory usage, and deployment costs.

Fortunately, thanks to the excellent language understanding and generation capabilities of LLMs, it is promising to input different task requirements to LLMs with natural language and thus to facilitate performing multiple tasks with one network. Therefore, in this work, we make the initial attempt to propose a LLM-enabled multi-task physical layer network to *unify* multiple tasks with a *single* LLM. To be specific, firstly, leveraging the global feature extraction and reasoning ability of LLMs, a multi-task LLM framework is proposed, which finetunes LLM to perform multi-user precoding, signal detection and channel prediction simultaneously. Secondly, to cope with different tasks and different data formats of the tasks, we elaborately design multi-task instructions as prompts of LLM; besides, to bridge the gap between the feature of wireless data and that of the LLM, task-specific encoders and decoders are proposed to adapt the text-based

This work was funded in part by the National Science Fund for Distinguished Young Scholars (Grant No. 62325106), and in part by the National Key R&D Program of China (No. 2023YFB811503).

T. Zheng, and L. Dai are with the Department of Electronic Engineering, Tsinghua University, Beijing 100084, China, and also with the Beijing National Research Center for Information Science and Technology (BNRist), Beijing 100084, China (e-mails: zhengty22@mails.tsinghua.edu.cn, daill@tsinghua.edu.cn).

pre-trained LLM. Last but not least, simulation results verified the effectiveness of the proposed method, which achieves comparable performance with dedicated designed network for each task.

Notation: \mathbf{a}^H , \mathbf{A}^H denote the conjugate transpose of vector \mathbf{a} and matrix \mathbf{A} , respectively; $\|\mathbf{a}\|_2$ denotes the l_2 norm of vector \mathbf{a} ; $\|\mathbf{A}\|_F$ denotes the Frobenius norm of matrix \mathbf{A} ; \mathbb{R}, \mathbb{C} denote the set of real numbers and complex numbers, respectively; $\mathcal{CN}(\mu, \Sigma)$ denotes the probability density function of complex multivariate Gaussian distribution with mean μ and variance Σ .

II. SYSTEMS MODEL

We consider a multi-user (MU) multiple input single output (MISO)- orthogonal frequency division multiplexing (OFDM) system, where a base station (BS) simultaneously serves K single-antenna moving users with K RF chains. The BS is equipped with a uniform planar array (UPA) with $N_T = N_h \times N_v$ antennas, where N_h and N_v represent the number of antennas in the horizontal and vertical directions, respectively. To design a multi-task LLM for the BS, we select three typical tasks in physical layer communications in different scenarios for instance, namely downlink multi-user precoding, uplink signal detection and channel prediction for moving conditions, respectively. Then, we will briefly illustrate the system models and formulate the tasks sequentially. Note that we use a for downlink transmission while \bar{a} for uplink transmission.

A. Multi-user Precoding

For downlink transmission scenario, the channel between user k and the BS at the m -th subcarrier is denoted as $\mathbf{h}_k^m \in \mathbb{C}^{N_t \times 1}$, $m = 1, 2, \dots, M$. The received signal at user k at the m -th subcarrier is given by

$$y_k^m = \mathbf{h}_k^{mH} \sum_{k'=1}^K \mathbf{w}_{k'}^m x_{k'}^m + n_k^m, \quad (1)$$

where \mathbf{w}_k^m represents the beamforming vector for user k , $x_k^m \sim \mathcal{CN}(0, 1)$ is the transmitted symbol from the BS to user k , and $n_k^m \sim \mathcal{CN}(0, \sigma^2)$ denotes the additive Gaussian white noise (AWGN) with zero mean and variance σ^2 .

Multi-user precoding aims to optimize the transmit beamformers such that the system sum-rate is maximized subject to a total power constraint due to the BS power budget. For simplicity, we design the beamformers based on the channel of the central carrier-frequency \mathbf{h}_k and the problem is mathematically formulated as

$$\mathbf{P1:} \max_{\mathbf{W}} \sum_{k=1}^K \log_2(1 + \gamma_k), \quad \text{s.t.} \quad \sum_{k=1}^K \|\mathbf{w}_k\|^2 \leq P_{\max}, \quad (2)$$

where $\mathbf{W} = [\mathbf{w}_1, \mathbf{w}_2, \dots, \mathbf{w}_K]$ is a set of beamforming vectors and P_{\max} is the power budget. Besides, γ_k represents the received signal-to-interference-plus-noise ratio (SINR) at user k , which is written as

$$\gamma_k = \frac{|\mathbf{h}_k^H \mathbf{w}_k|^2}{\sum_{k'=1, k' \neq k}^K |\mathbf{h}_k^H \mathbf{w}_{k'}|^2 + \sigma^2}. \quad (3)$$

As pointed out in [19] that the optimal downlink beamforming vectors for problem **P1** follows the structure as

$$\mathbf{w}_k^* = \sqrt{p_k} \frac{\left(\mathbf{I}_{N_T} + \sum_{k=1}^K \frac{\lambda_k}{\sigma^2} \mathbf{h}_k \mathbf{h}_k^H \right)^{-1} \mathbf{h}_k}{\left\| \left(\mathbf{I}_{N_T} + \sum_{k=1}^K \frac{\lambda_k}{\sigma^2} \mathbf{h}_k \mathbf{h}_k^H \right)^{-1} \mathbf{h}_k \right\|_2}, \quad \forall k, \quad (4)$$

where λ_k is a positive parameter and $\sum_{k=1}^K \lambda_k = \sum_{k=1}^K p_k = P_{\max}$. The solution structure in (4) provides the required expert knowledge for the beamforming design in problem **P1**. Therefore, the network is only required to learn the key features $\lambda = [\lambda_1, \lambda_2, \dots, \lambda_K]$ and $\mathbf{p} = [p_1, p_2, \dots, p_K]$.

B. Signal Detection

During uplink transmission, the BS receiver antennas simultaneously receive the transmitted symbols from the K users. Denote the transmitted symbol vector from four users at the m -th subcarrier as $\bar{\mathbf{x}}^m = [\bar{x}_1^m, \bar{x}_2^m, \dots, \bar{x}_K^m] \in \mathbb{C}^{K \times 1}$. Each element is drawn from the P -QAM constellation, and then transmitted over channel. The received signal $\bar{\mathbf{y}}^m \in \mathbb{C}^{N_T \times 1}$ is given by

$$\bar{\mathbf{y}}^m = \bar{\mathbf{H}}^m \bar{\mathbf{x}}^m + \bar{\mathbf{n}}^m, \quad (5)$$

where $\bar{\mathbf{H}}^m = [\bar{\mathbf{h}}_1^m, \bar{\mathbf{h}}_2^m, \dots, \bar{\mathbf{h}}_K^m]$ is the uplink channel of the K users and $\bar{\mathbf{n}}^m \sim \mathcal{CN}(0, \sigma^2 \mathbf{I}_{N_T})$ is the AWGN at the m -th subcarrier.

BS requires to recover the signals $\bar{\mathbf{x}}^m$ from the received signal $\bar{\mathbf{y}}^m$ given $\bar{\mathbf{H}}^m$. In this work, we adopt the minimum mean squared error (MMSE) estimator and the problem can be formulated as

$$\mathbf{P2:} \min_{\Omega_{\text{DEC}}} \min \|\hat{\bar{\mathbf{x}}}^m - \bar{\mathbf{x}}^m\|_2 \quad (6)$$

$$\text{s.t.} \quad \hat{\bar{\mathbf{x}}}^m = f_{\Omega_{\text{DEC}}}(\bar{\mathbf{H}}^m, \bar{\mathbf{y}}^m), \quad (7)$$

where $f_{\Omega_{\text{DEC}}}$ is the mapping function with variable parameters Ω_{DEC} .

C. Channel Prediction

In mobile scenarios involving high-velocity users, it is possible that the channel coherence time is shorter than the channel estimation period. In such cases, accurate channel prediction is vital to address the channel aging issue [20] in mobile communications with fast time-varying channels. In this work, we aim to accurately predict future channel state information (CSI) of T_2 time slots based on historical CSI of T_1 time slots. The CSI of M subcarriers at time t is represented in matrix form as

$$\mathbf{H}_k^t = [\mathbf{h}_k^{1,t}, \mathbf{h}_k^{2,t}, \dots, \mathbf{h}_k^{M,t}], \quad \forall k, t, \quad (8)$$

where $\mathbf{h}_k^{m,t}$ is the channel of user k , time t , and subcarrier m .

The normalized MSE (NMSE) between predicted and actual future CSI is employed to evaluate the prediction accuracy. Then the entire problem can be described as follows:

$$\mathbf{P3:} \min_{\Omega_{\text{CP}}} \frac{\sum_{t=1}^{T_2} \|\hat{\mathbf{H}}^{t_0+t} - \mathbf{H}^{t_0+t}\|_F^2}{\sum_{t=1}^{T_2} \|\mathbf{H}^{t_0+t}\|_F^2} \quad (9)$$

$$\text{s.t.} \quad (\hat{\mathbf{H}}^{t_0+1}, \dots, \hat{\mathbf{H}}^{t_0+T_2}) = f_{\Omega_{\text{CP}}}(\mathbf{H}^{t_0}, \dots, \mathbf{H}^{t_0-T_1+1}), \quad (10)$$

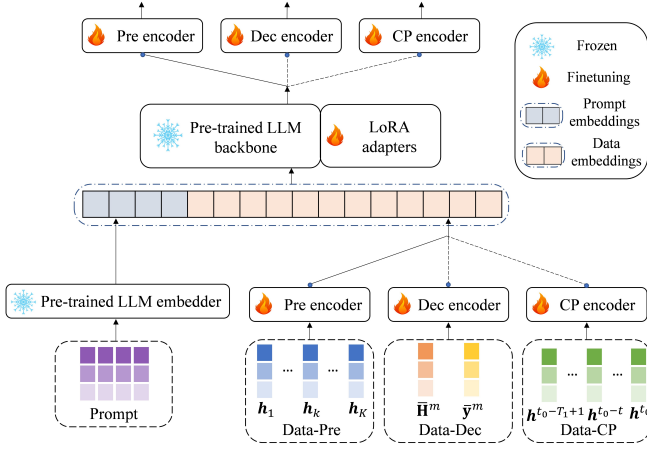


Fig. 1. The model framework of our method.

where $\hat{\mathbf{H}}^t$ is the predicted CSI, and $f_{\Omega_{CP}}$ is the constructed mapping function and Ω_{CP} is its variable parameters. Note here we ignore the subscript since the channel prediction is performed independently to each user.

III. PROPOSED PHYSICAL LAYER MULTI-TASK LLM

In this section, we propose an LLM-empowered physical layer network to *unify multiple tasks* (channel prediction, multi-user precoding, as well as signal detection) with a *single* network. The proposed framework is illustrated in Fig. 1, including multi-task instruction module, input encoder, LLM backbone, and output decoder. We describe each component, together with the training schedule as follows.

A. Multi-task Instruction Template

When training a single unified model for multiple different tasks, a basic and critical problem is how to distinguish each task. Fortunately, thanks to the remarkable text understanding capability, LLM allows users to input task requirements with natural language. Therefore, we design multi-task instruction template with task specific tokens as prompt to make each task easily distinguishable. Next, we introduce our multi-task instruction template in details.

We structure the instruction template into three parts, which is denoted as follows,

$$[\textit{Task Identifier}]\textit{Task description} \langle \textit{Instruction} \rangle. \quad (11)$$

The first part is the task identifier token, the second part is the task and data description, and the third part is the instruction input. **Task Identifier** provides a distinct identifier for each task to reduce the ambiguity across various tasks. **Task description** attempts to input basic domain knowledge and illustrate the dataset for LLM to better understand the task. Take multi-user precoding as an example, the designed task description is presented by “Multi-user precoding aims to maximize the sum rate of multiple users through the design of base station precoder, to serve multiple users using a single base station. For the collected dataset, we consider a base

station with 4 RF chains and 128 antennas to serve 4 single antenna user simultaneously.”. The third part **Instruction** gives direct and clear objective of the task. Again, for instance the instruction for multi-user precoding is “<Instruction> Design the precoding matrix given channels of the users, to maximize the sum rate of the multiple users.”.

The designed prompt is then fed to the pre-trained LLM embedder to adapt to the input format of LLM. The prompt embedding is denoted as $\mathbf{X}_{\text{prompt}}^{\text{emb}}$.

B. Input Encoders

Adapting text-based pre-trained LLM to multiple communication domain tasks is another challenging problem. To be specific, firstly, there is a huge gap between specific characteristics of communication domain data and the natural language. Therefore, directly applying a general-domain LLM to these tasks may lead to poor performance. Secondly, the format, length and meaning of the data also differs significantly among the tasks. The difficulties urge us to design dedicated input encoder modules for each task to fit for the feature space of the LLM, and facilitate multi-task feature extraction.

1) *Encoder for multi-user precoding*: Since neural networks generally deal with real numbers, we first convert the complex multi-user channel into real tensors $\mathbf{X}_{\text{Pre}}^{\text{in}} \in \mathbb{R}^{K \times 2N_t}$ as the input. For multi-user precoding, we employ a transformer to extract the channel feature and inter-user relationship. The transformer is composed of $L = 3$ blocks, the structure of which is presented in Fig. 2, including a multi-head self-attention module and a multilayer perceptron (MLP) module. The input $\mathbf{X}_{\text{Pre}}^{\text{in}}$ is first processed by the multi-head self-attention module:

$$\mathbf{X}_{\text{Pre}}^{\text{att}(1)} = \text{LayerNorm}(\text{ATT}(\mathbf{X}_{\text{Pre}}^{\text{in}}) + \mathbf{X}_{\text{Pre}}^{\text{in}}), \quad (12)$$

where $\text{ATT}(\cdot)$ denotes the multi-head self-attention. Then MLP module is performed as

$$\mathbf{X}_{\text{Pre}}^{\text{mlp}(1)} = \text{LayerNorm}(\text{MLP}(\mathbf{X}_{\text{Pre}}^{\text{att}(1)}) + \mathbf{X}_{\text{Pre}}^{\text{att}(1)}), \quad (13)$$

which serves as the input of next block. Denote the output of the transformer as $\mathbf{X}_{\text{Pre}}^{\text{mlp}(3)}$, and then a linear projection layer projects $\mathbf{X}_{\text{Pre}}^{\text{mlp}(3)}$ into the language model space

$$\mathbf{X}_{\text{Pre}}^{\text{emb}} = \text{Linear}(\mathbf{X}_{\text{Pre}}^{\text{mlp}(3)}). \quad (14)$$

2) *Encoder for signal detection*: The input of signal detection contains the uplink channel $\bar{\mathbf{H}}^m$ and the received signal $\bar{\mathbf{y}}^m$. The encoder rearranges the channel $\bar{\mathbf{H}}^m$ as one token $\mathbf{X}_{\text{Dec}}^{\text{Hin}} \in \mathbb{R}^{1 \times 2KN_t}$. Then a MLP module is employed to extract features from the channel

$$\mathbf{X}_{\text{Dec}}^{\text{Hmlp}} = \text{MLP}(\mathbf{X}_{\text{Dec}}^{\text{Hin}}). \quad (15)$$

We also extract shallow features from the rearranged real received signal $\mathbf{X}_{\text{Dec}}^{\text{yin}}$ by a MLP module

$$\mathbf{X}_{\text{Dec}}^{\text{ympl}} = \text{MLP}(\mathbf{X}_{\text{Dec}}^{\text{yin}}). \quad (16)$$

In the simulation parts, we find that integrating received signals of several time slots into one sample effectively improves the training performance compared to treating them as multiple

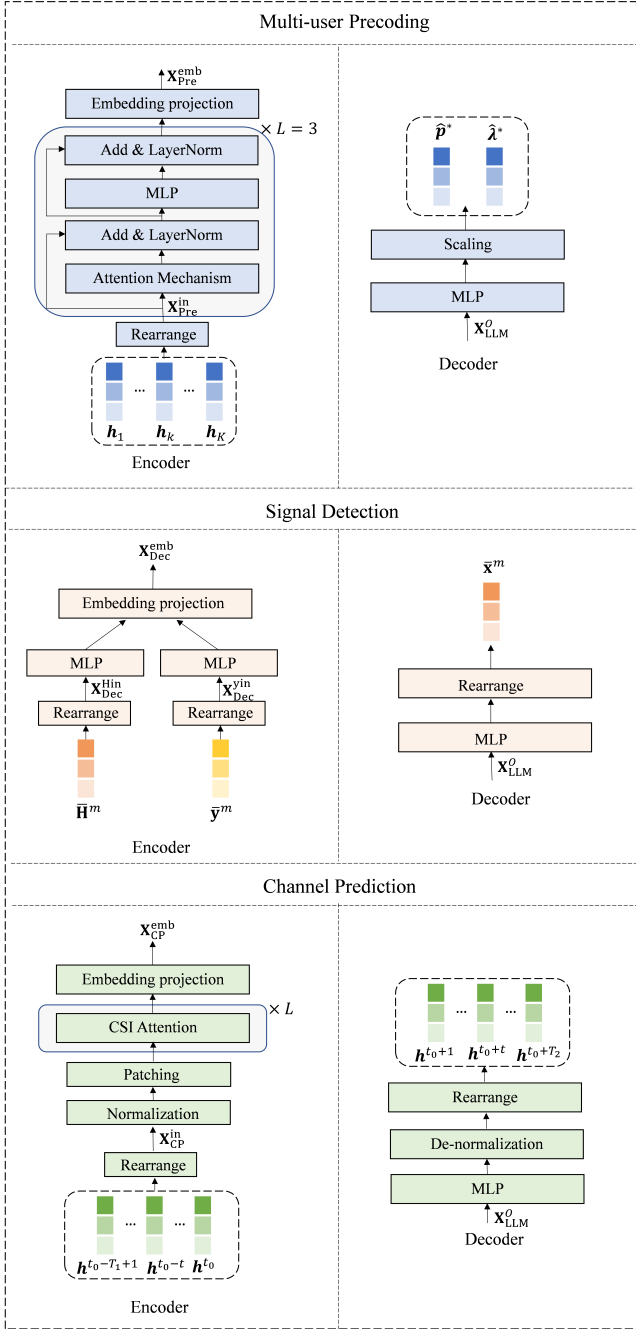


Fig. 2. Detailed illustration of encoders and decoders.

samples. Therefore, we utilize received signals of $L_0 = 8$ time slots in one sample in practice. Then, the extracted features of channel and received data are concatenated and projected to the input format of LLM:

$$\mathbf{X}_{\text{Dec}}^{\text{emb}} = \text{Linear}([\mathbf{X}_{\text{Dec}}^{\text{Hmlp}}, \mathbf{X}_{\text{Dec}}^{\text{ymlp}}]). \quad (17)$$

3) *Encoder for channel prediction:* Consider that the CSI $\mathbf{H}^t \in \mathbb{C}^{N_t \times M}$ of at time t is the high-dimensional structural data, directly predicting the matrix by the network will bring significant complexity and training time, especially for a

large number of antennas and subcarriers. Inspired by [16], we parallelize the processing of antennas, i.e., predicting the CSI for each transmitter antenna separately. Thereby, the input sample of j -th $\forall j$ antenna can be converted into real tensors and rearranged to merge feature dimensions as $\mathbf{X}_{\text{CP}}^{\text{in}} \in \mathbb{R}^{T_1 \times 2M}$. To facilitate network training and convergence, we first normalize the input data as $\mathbf{X}_{\text{CP}}^{\text{in}} = \frac{\mathbf{X}_{\text{CP}}^{\text{in}} - \mu_{\text{CP}}}{\sigma_{\text{CP}}}$, where $(\mu_{\text{CP}}, \sigma_{\text{CP}})$ represent the mean value and standard deviation of a batch of corresponding domain input data. To capture the local temporal features and reduce computational complexity, patching operation along the temporal dimension is adopted. Specifically, $\mathbf{X}_{\text{CP}}^{\text{in}}$ are grouped into non-overlapping patches of size N as $\mathbf{X}_{\text{CP}}^{\text{pat}} \in \mathbb{R}^{T_1' \times N \times 2M}$ [21], where $T_1' = \lceil \frac{T_1}{N} \rceil$ is the number of patches. Zero-padding is applied to the last patch that is not fully filled. We adopt the CSI attention module, which is proposed and described in detail in [22], to extract preliminary temporal and frequency features before LLM. The process can be presented by

$$\mathbf{X}_{\text{CP}}^{\text{CA}} = \text{CSIATT}^L(\mathbf{X}_{\text{CP}}^{\text{pat}}), \quad (18)$$

where CSIATT^L represents the CSI attention module cascaded L times. Finally, to adapt to the input format of LLM, $\mathbf{X}_{\text{CP}}^{\text{CA}}$ is rearranged to $\mathbf{X}_{\text{CP}}^{\text{CA}'} \in \mathbb{R}^{T_1' \times 2MN}$ and then mapped to the feature dimension of the pre-trained LLM with a single fully-connected layer:

$$\mathbf{X}_{\text{CP}}^{\text{emb}} = \text{Linear}(\mathbf{X}_{\text{CP}}^{\text{CA}'}). \quad (19)$$

C. LLM Mainbody with Low-rank Adaptation (LoRA)

The proposed method finetunes LLM by a parameter-efficient technique, low-rank adaptation (LoRA) [23], which freezes the pre-trained model weights and injects trainable rank decomposition matrices into each layer. The use of LoRA mainly brings two advantages. Firstly, due to the immense parameter size of LLMs, full-parameter finetuning could be impractical. LoRA circumvents this by only fine-tuning low-rank adapters, with a significantly smaller number of parameters, yielding results comparable to full-parameter finetuning. Secondly, LoRA prevents catastrophic forgetting of the original knowledge, as the newly learned knowledge has a lower rank than the original knowledge. Therefore, it facilitates us to utilize the universal modeling and generalization capability of pre-trained LLMs to achieve multiple tasks with a single model.

Without loss of generality, LLAMA2 is chosen as the LLM backbone in this work. The backbone of LLAMA2 is composed of stacked transformer decoders, the structure of which is illustrated in Fig. 3. We focus on training the linear projection layer and efficient finetuning the LLM backbone using LoRA. With LoRA, we finetune W_q and W_v via low-rank adaptation. It is worth noting that in the proposed method, the backbone can be flexibly replaced with other LLM, such as GPT [10] or QWen [24]. The selection of the type and size of the LLM, as well as the rank and finetuned modules of LoRA, needs to consider the trade-off between training costs and performance.

Obtaining the LLM backbone, we concatenate the embedding of prompt and data obtained in the previous subsections

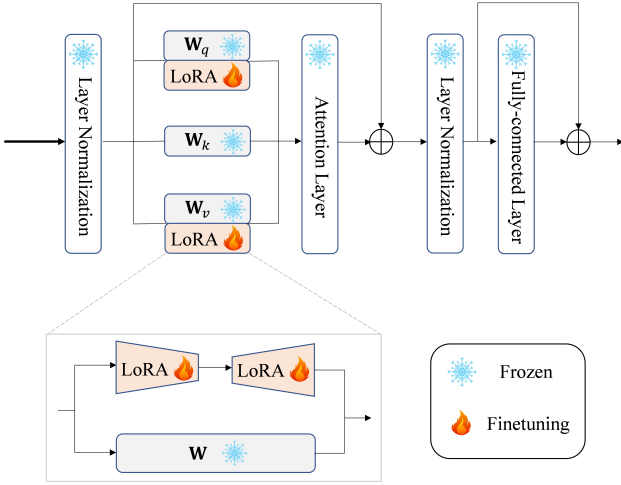


Fig. 3. The illustration of LoRA adapters.

as \mathbf{X}^{emb} and feed into the LLM backbone. The output can be obtained by

$$\mathbf{X}_{\text{LLM}}^O = \text{LLM}(\mathbf{X}^{\text{emb}}). \quad (20)$$

D. Output Decoders

Similar to input encoders, to facilitate multiple downstream tasks simultaneously, task-specific decoders are required to be designed to convert the output features of the LLM into the final results for different tasks. Then we elaborate on the output decoders of the three tasks sequentially. Note that for output decoders, we discard the prefix portion and retain only the output presentations of the data for the decoder.

1) *Decoder for multi-user precoding*: As discussed in Section II A., the multi-user precoding problem can be transformed into learning the key features $\lambda = [\lambda_1, \lambda_2, \dots, \lambda_K]$ and $\mathbf{p} = [p_1, p_2, \dots, p_K]$. Therefore, a MLP module comprising of two fully-connected (FC) layers is adopted to generate $2K$ values including the power allocation vectors $\hat{\lambda}$ and $\hat{\mathbf{p}}$. The output of the MLP module $\mathbf{X}_{\text{Pre}}^O \in \mathbb{R}^{K \times 2}$ can be written as

$$\mathbf{X}_{\text{Pre}}^O = \text{MLP}(\mathbf{X}_{\text{LLM}}^O), \quad (21)$$

where $\hat{\lambda} = \mathbf{X}_{\text{Pre}}^O[:, 1]$ and $\hat{\mathbf{p}} = \mathbf{X}_{\text{Pre}}^O[:, 2]$. Then the scaling layer scales the results of the output layer $\hat{\lambda}$ and $\hat{\mathbf{p}}$ to meet the power constraint by the following method:

$$\hat{\mathbf{p}}^* = \frac{P_{\max}}{\|\hat{\mathbf{p}}\|_1} \hat{\mathbf{p}} \quad \text{and} \quad \hat{\lambda}^* = \frac{P_{\max}}{\|\hat{\lambda}\|_1} \hat{\lambda}. \quad (22)$$

2) *Decoder for signal detection*: For signal detection, we employ two FC layers to transform the dimension of the $\mathbf{X}_{\text{LLM}}^O$ to the antenna number:

$$\mathbf{X}_{\text{Dec}}^{\text{mlp}} = \text{MLP}(\mathbf{X}_{\text{LLM}}^O). \quad (23)$$

Then $\mathbf{X}_{\text{Dec}}^{\text{mlp}}$ is rearranged $\mathbf{X}_{\text{Dec}}^O \in \mathbb{R}^{K \times 2}$ to where the first and the second dimension respectively correspond to the real part and the imaginary part.

3) *Decoder for channel prediction*: For convenience, we also utilize a simple MLP module as the decoder to predict

the channel. The output is presented by

$$\mathbf{X}_{\text{CP}}^{\text{mlp}} = \text{MLP}(\mathbf{X}_{\text{LLM}}^O). \quad (24)$$

Then $\mathbf{X}_{\text{CP}}^{\text{mlp}}$ is de-normalized to generate the final output of the network, i.e.,

$$\mathbf{X}_{\text{CP}}^{\text{norm}} = \sigma_{\text{CP}} \mathbf{X}_{\text{CP}}^{\text{mlp}} + \mu_{\text{CP}}. \quad (25)$$

Then the tensors are rearranged to $\mathbf{X}_{\text{CP}}^O \in \mathbb{R}^{T_2 \times M \times 2}$ to separate the real part and the imaginary part of the predicted channel.

E. Multi-task Loss Function and Training Schedule

During the training stage, we randomly choose a task and sample data from the corresponding dataset for each iteration. After determining the involved task and data, we select the proper prompt and activate the required modules of encoder and decoder. It is worth noting that the backbone of the pre-trained LLM is frozen, while the other parameters of the network, together with the LoRA adapters are trainable. Then the proposed network update the parameters of encoders, decoders and LoRA adapters using the corresponding loss. Next, we will illustrate the loss function of the tasks, respectively.

For **multi-user precoding**, the training is divided into two stages, namely supervised learning and unsupervised learning, respectively. The WMMSE algorithm is one of the most popular iterative to find the locally optimal solutions. Therefore, in the supervised learning stage, we can obtain the power allocation vectors $\underline{\mathbf{p}}$ and $\underline{\lambda}$ according to the WMMSE algorithm as the label. Then the supervised learning with the loss function based on the MSE metric will be first used to achieve as close to the results of the WMMSE algorithm as possible, i.e.,

$$\text{Loss}_{Pre} = \frac{1}{2K} \left(\|\underline{\mathbf{p}} - \hat{\mathbf{p}}^*\|_2^2 + \|\underline{\lambda} - \hat{\lambda}^*\|_2^2 \right), \quad (26)$$

where $\underline{\mathbf{p}}$ and $\underline{\lambda}$ are the power vectors obtained from the WMMSE algorithm. However, the WMMSE algorithm is locally optimal and thus (26) is not equivalent to the real objective of problem **P3** which aims to maximize the weighted sum rate. To further improve the sum rate performance, we continue to train the network in an unsupervised learning way, whose loss function takes the objective function directly as a metric, i.e.,

$$\text{Loss}_{Pre} = - \sum_{k=1}^K \log_2(1 + \gamma_k) \quad (27)$$

In the **signal detection** task, the original transmitted data is rearranged as $\mathbf{X}_{\text{Dec}} \in \mathbb{R}^{K \times 2}$, which serves as ground truth of the network output. Then we choose MSE loss for the training phase,

$$\text{Loss}_{Dec} = \frac{1}{2K} \|\mathbf{X}_{\text{Dec}} - \mathbf{X}_{\text{Dec}}^O\|_F^2. \quad (28)$$

For **channel prediction**, the ground truth of the predicted CSI is also available. We transform the complex CSI matrix to real ground truth $\mathbf{X}_{\text{CP}} \in \mathbb{R}^{T_2 \times M \times 2}$, and MSE is adopted

as the loss function to minimize the prediction error, i.e.,

$$\text{Loss}_{CP} = \frac{1}{2MT_2} \|\mathbf{X}_{CP} - \mathbf{X}_{CP}^O\|_F^2. \quad (29)$$

IV. SIMULATION RESULTS

A. Simulation Setup

In the simulation parts, we adopt the widely used channel generator QuaDRiGa [25], where we consider the 3GPP Urban Macro (UMa) channel model [26] and non-line-of-sight (NLOS) scenarios. The number of clusters is 21 and the number of paths per cluster is 20. We consider a multi-user MISO-OFDM system, where a BS simultaneously serves $K = 4$ moving users. BS is equipped with a UPA with $N_h = 16$, $N_v = 8$ while each user is equipped with a single omnidirectional antenna. The antenna spacing is half of the wavelength at the center frequency. The users are uniformly distributed within angle range $[-\pi/2, \pi/2]$, and distance range $[\rho_{\min}, \rho_{\max}] = [20 \text{ m}, 100 \text{ m}]$. We suppose a time-division duplex (TDD) system, where the center frequency of channel is set as 2.4 GHz. The bandwidth of the channel is 8.64 MHz, comprising of $M = 48$ subcarriers, i.e., the frequency interval of subcarriers is 180 kHz. The training dataset and test dataset respectively contain 90000 and 10000 samples for each task.

For channel prediction problem, We predict future CSI of $T_2 = 4$ time slots based on historical CSI of $T_1 = 16$ time slots and set the time interval of pilots as 0.5 ms. The initial position of the user is randomized and the motion trajectory is set as linear type. The user velocities are uniformly distributed between 10 and 100 km/h. For uplink signal detection, we suppose the transmitted data is generated from 16-QAM modulation symbol.

B. Performance Evaluation for Channel Prediction

1) *Baselines and Performance Metric*: To evaluate the performance, we compare the proposed multi-task LLM with the following benchmarks.

- **Transformer**: In [5], a transformer-based parallel channel predictor is proposed scheme to predict future channels in parallel, and thus avoid error propagation problems.
- **RNN**: A Recurrent Neural Network (RNN) [27] is a traditional type of neural network used for processing sequences and is commonly utilized in channel prediction tasks. In the experiments, we configure the RNN with four layers.
- **LSTM**: Long short-term memory (LSTM) [28] is designed with memory cells and multiplicative gates to deal with long-term dependency. An LSTM-based predictor with 4 LSTM layers is applied.
- **GRU**: Gate recurrent unit (GRU) [29] is a variant of LSTM to address the vanishing gradient problem. Similarly, the number of GRU layers is set as 4 for channel prediction.
- **LLM4CP**: [16] first attempts to propose a pre-trained LLM-empowered channel prediction method (LLM4CP) based on GPT-2 to achieve improved predictive capability and generalization ability.

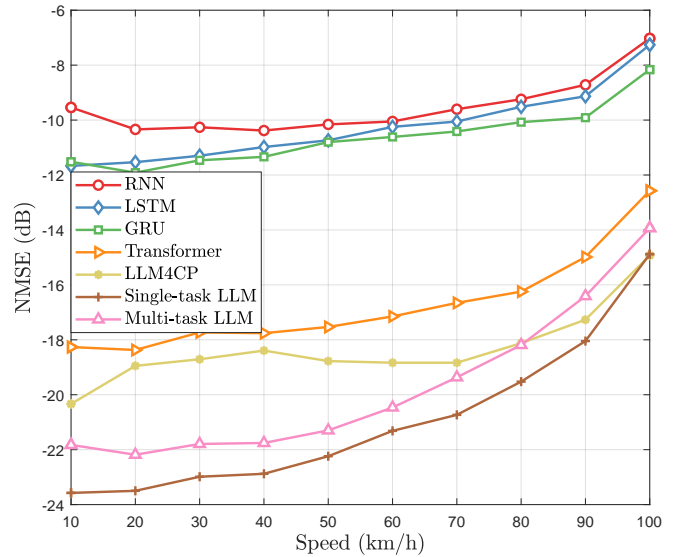


Fig. 4. The NMSE performance of proposed method and other baselines versus different user velocities.

- **Single-task LLM**: We also train the proposed network on a single task to better analyze the performance.

For channel prediction task, NMSE is a widely used performance metric to directly characterize the accuracy of channel prediction. Therefore, NMSE is adopted as a major metric in our experiments.

2) *Performance Analysis*: The testing dataset of channel prediction contains 10 velocities ranging from 10 km/h to 100 km/h, with 1000 samples for each velocity. Fig. 4 reveals the NMSE performance of the proposed multi-task LLM with other baselines among different user velocities. It can be observed that as the user velocity increases, the NMSE of all baselines gradually increases. This is due to that as the user velocity increases, the CSI changes rapidly with a shorter channel coherence time, resulting in increased prediction difficulty. As illustrated in Fig. 4, attention-based methods, achieve relatively high-performance than traditional AI methods, validating the potential of attention-based method in channel prediction task. Equipped with excellent modeling capability of LLM, the proposed model finetuned on channel prediction task only, consistently outperforms other baselines among testing velocities. With elaborately designed multi-task instruction, the proposed LLM-enabled multi-task model obtains comparable channel prediction accuracy with single-task one, which verified the effectiveness of the proposed multi-task LLM.

C. Performance Evaluation for Multi-user Precoding

1) *Baselines and Performance Metric*: For multi-user precoding, the following methods are selected as baselines, including traditional methods and deep learning-based methods.

- **ZF**: A low complexity baseline is eigen-based zero-forcing (ZF) algorithm [30], which obtains the precoding matrix by the Moore-Penrose pseudo-inverse of the channel.

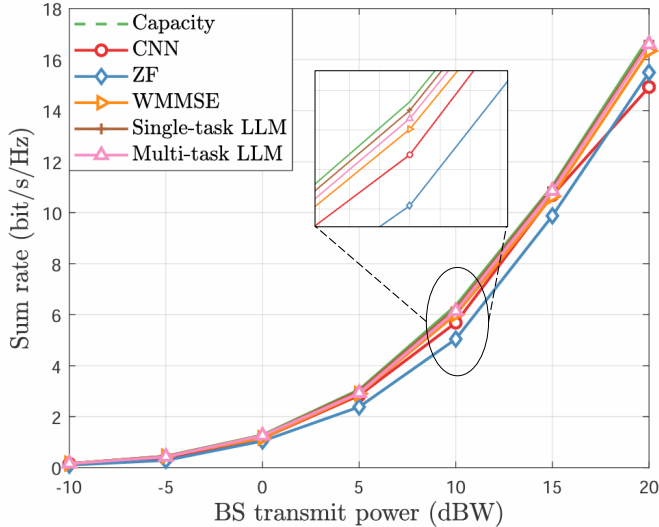


Fig. 5. The sum rate performance of proposed method and other baselines versus different BS transmit powers.

- WMMSE: As mentioned above, the WMMSE algorithm [31] is one of the most popular iterative algorithms. The method can achieve near optimal sum rate performance while suffers from high computational complexity. The iterative number is set as 20.
- CNN: In [32], the authors propose a CNN-based framework for the optimization of downlink beamforming.
- Single-task LLM: Similarly, we train the proposed network on multi-user precoding only.

The sum rate of users, which is the objective of multi-user precoding, is utilized as performance metric to evaluate the multi-user precoding task.

2) *Performance Analysis*: The sum rate performance against different BS transmit power is plotted in Fig. 5. The noise power is set as $\sigma^2 = -20$ dBW, the maximal transmit power of BS P_{\max} increases from -10 to 20 dBW. The ZF-based method and CNN-based method, though with low complexity, achieves unsatisfactory performance. The iterative algorithm WMMSE improves the sum rate, while it is still possible to fall in local optimal solutions. As depicted in Fig. 5, the proposed model, both trained on single task and trained on multiple tasks, achieves near-optimal performance for all the transmit powers, and outperforms other baselines.

D. Performance Evaluation for Signal Detection

1) *Baselines and Performance Metric*: To validate the effectiveness of the proposed method, several methods are implemented as baselines.

- LMMSE: Linear minimum mean-squared error (LMMSE) detectors are a classical method for achieving signal detection with low complexity.
- DNN: In [33], a data-driven model which inputs the channel as well as the received data and outputs the original data through a deep learning network.

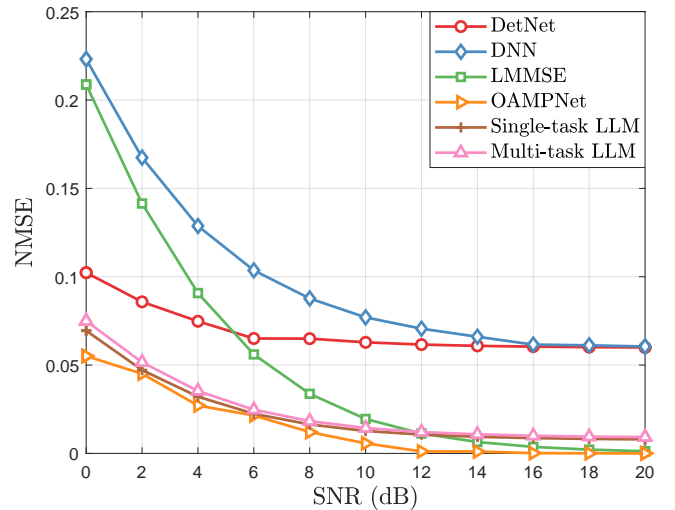


Fig. 6. The NMSE performance of proposed method and other baselines versus different SNRs.

- DetNet: The detection network (DetNet) in [34] unfolds the iterations of a projected gradient descent algorithm to recover the data.
- OAMP-Net: A famous model-driven deep learning network proposed in [6], which incorporates deep learning into the orthogonal AMP (OAMP) algorithm.
- Single-task LLM: The proposed network is finetuned only on the signal detection task.

NMSE loss is the direct performance metric to present the accuracy of data recovery. It should be noted that the reason for choosing the data recovery accuracy rather than the bit error ratio (BER) or symbol error ratio (SER) to optimize and evaluate the model is described below. In the practical communication link, the objective of signal detection is to recover the data as accurately as possible, which can be utilized to compute the log-likelihood ratio (LLR) for demodulation and channel decoding to enable reliable communications. Thus, we utilized the NMSE to evaluate the performance of signal detection.

2) *Performance Analysis*: In Fig. 6, the NMSE performance of the proposed multi-task LLM on signal detection is presented. We also compare the performance with several baselines. The OAMPNet [6] achieves the best performance since it fully utilizes the statistical information of noise, which may not be obtained in practical system. Moreover, the proposed multi-task LLM can accurately recover the transmitted data, especially in low SNR regime. It can be observed that the performance of multi-task LLM is comparable to that of single-task LLM, suggesting the potential of multi-task LLM. Besides, the proposed method achieves high robustness in low SNR regime.

V. CONCLUSIONS

In this paper, we propose a LLM-enabled multi-task physical layer network to unify multiple tasks with a single LLM. Multi-task instruction module, input encoders, as well as output decoder, are elaborately designed to distinguish multiple

tasks and adapted the features of different formats of wireless data for the feature of LLM. Simulation results have verified the effectiveness of the proposed method. The proposed LLM framework is promising to perform different tasks according to the requirements with a single model, significantly saving the redundancy and costs of designing LLM for each task separately. Future works can be focused on incorporating more tasks into the network.

REFERENCES

- [1] J. Hoydis, F. A. Aoudia, A. Valcarce, and H. Viswanathan, "Toward a 6G ai-native air interface," *IEEE Commun. Mag.*, vol. 59, no. 5, pp. 76–81, 2021.
- [2] T. O'Shea and J. Hoydis, "An introduction to deep learning for the physical layer," *IEEE Trans. Cog. Commun. Netw.*, vol. 3, no. 4, pp. 563–575, 2017.
- [3] C.-K. Wen, W.-T. Shih, and S. Jin, "Deep learning for massive MIMO CSI feedback," *IEEE Wireless Commun. Lett.*, vol. 7, no. 5, pp. 748–751, 2018.
- [4] H. He, C.-K. Wen, S. Jin, and G. Y. Li, "Deep learning-based channel estimation for beamspace mmwave massive MIMO systems," *IEEE Wireless Commun. Lett.*, vol. 7, no. 5, pp. 852–855, 2018.
- [5] H. Jiang, M. Cui, D. W. K. Ng, and L. Dai, "Accurate channel prediction based on transformer: Making mobility negligible," *IEEE J. Sel. Areas Commun.*, vol. 40, no. 9, pp. 2717–2732, 2022.
- [6] H. He, C.-K. Wen, S. Jin, and G. Y. Li, "Model-driven deep learning for mimo detection," *IEEE Trans. Signal Process.*, vol. 68, pp. 1702–1715, 2020.
- [7] M. K. Shehzad, L. Rose, M. M. Butt, I. Z. Kovács, M. Assaad, and M. Guizani, "Language models are unsupervised multitask learners," *IEEE Veh. Tech. Mag.*, vol. 17, no. 3, pp. 16–25, 2022.
- [8] R. K. Alec, J. Wu, R. Child, D. Luan, D. Amodei, and I. Sutskever, "Language models are unsupervised multitask learners," *OpenAI blog*, vol. 1, no. 8, p. 9, 2019.
- [9] H. Touvron, L. Martin, K. R. Stone, P. Albert, A. Almahairi, Y. Babaei, N. Bashlykov, S. Batra, P. Bhargava, and *et al.*. Shrutí Bhosale, "Llama 2: Open foundation and fine-tuned chat models," *arXiv preprint arXiv:2307.09288*, 2023.
- [10] T. Brown, B. Mann, N. Ryder, M. Subbiah, J. D. Kaplan, P. Dhariwal, A. Neelakantan, P. Shyam, G. Sastry, and *et al.*. Amanda Askell, "Language models are few-shot learners," in *Proc. Adv. Neural Inf. Process. Syst. (NeurIPS)*, Dec. 2020, pp. 1–5.
- [11] J. Shao, J. Tong, Q. Wu, W. Guo, Z. Li, Z. Lin, and J. Zhang, "Wirelessllm: Empowering large language models towards wireless intelligence," *J. Commun. Info. Netw.*, vol. 9, no. 2, pp. 99–112, 2024.
- [12] H. Zhou, C. Hu, Y. Yuan, Y. Cui, Y. Jin, C. Chen, H. Wu, D. Yuan, L. Jiang, and *et al.*. Wu, Di, "Large language model (LLM) for telecommunications: A comprehensive survey on principles, key techniques, and opportunities," *IEEE Commun. Surv. Tutor.*, pp. 1–1, 2024.
- [13] W. Yu, H. He, S. Song, J. Zhang, L. Dai, L. Zheng, and K. B. Letaief, "AI and deep learning for THz ultra-massive MIMO: From model-driven approaches to foundation models," *arXiv preprint arXiv:2412.09839*, 2024.
- [14] F. Jiang, Y. Peng, L. Dong, K. Wang, K. Yang, C. Pan, D. Niyato, and O. A. Dobre, "Large language model enhanced multi-agent systems for 6G communications," *IEEE Wireless Communications*, vol. 31, no. 6, pp. 48–55, 2024.
- [15] L. Bariah, Q. Zhao, H. Zou, Y. Tian, F. Bader, and M. Debbah, "Large generative ai models for telecom: The next big thing?" *arXiv preprint arXiv:2306.10249*, 2023.
- [16] B. Liu, X. Liu, S. Gao, X. Cheng, and L. Yang, "LLM4CP: Adapting large language models for channel prediction," *J. Commun. Inf. Netw.*, vol. 9, no. 2, pp. 113–125, 2024.
- [17] Y. Sheng, K. Huang, L. Liang, P. Liu, S. Jin, and G. Y. Li, "Beam prediction based on large language models," *arXiv preprint arXiv:2408.08707*, 2024.
- [18] W. Lee and J. Park, "LLM-empowered resource allocation in wireless communications systems," *arXiv preprint arXiv:2408.02944*, 2024.
- [19] E. Björnson, M. Bengtsson, and B. Ottersten, "Optimal multiuser transmit beamforming: A difficult problem with a simple solution structure," *IEEE Signal Process. Mag.*, vol. 31, no. 4, pp. 142–148, 2014.
- [20] K. T. Truong and R. W. Heath, "Effects of channel aging in massive mimo systems," *J. Commun. Netw.*, vol. 15, no. 4, pp. 338–351, 2013.
- [21] Y. Nie, N. H. Nguyen, P. Sinthong, and J. Kalagnanam, "A time series is worth 64 words: Long-term forecasting with transformers," *arXiv preprint arXiv:2211.14730*, 2022.
- [22] J. Hu, L. Shen, and G. Sun, "Squeeze-and-excitation networks," in *2018 IEEE/CVF Conference on Computer Vision and Pattern Recognition (CVPR)*, 2018, pp. 7132–7141.
- [23] E. J. Hu, Y. Shen, P. Wallis, Z. Allen-Zhu, Y. Li, S. Wang, L. Wang, and W. Chen, "LoRA: low-rank adaptation of large language models," *arXiv preprint arXiv:2106.09685*, 2021.
- [24] A. Yang, B. Yang, B. Zhang, B. Hui, B. Zheng, B. Yu, C. Li, and *et al.*. Dayiheng Liu, "Qwen2.5 technical report," *arXiv preprint arXiv:2412.15115*, 2024.
- [25] S. Jaeckel, L. Raschkowski, K. Börner, and L. Thiele, "QuaDRiGa: A 3-d multi-cell channel model with time evolution for enabling virtual field trials," *IEEE Trans. Antennas and Propag.*, vol. 62, no. 6, pp. 3242–3256, 2014.
- [26] 3GPP RADIO ACCESS NETWORK WORKING GROUP, "Study on channel model for frequencies from 0.5 to 100 GHz(Release 15)[R]." 3GPP TR 38.901, 2018.
- [27] W. Jiang and H. D. Schotten, "Neural network-based fading channel prediction: A comprehensive overview," *IEEE Access*, vol. 7, pp. 118 112–118 124, 2019.
- [28] —, "Deep learning for fading channel prediction," *IEEE Open J. Commun. Soc.*, vol. 1, pp. 320–332, 2020.
- [29] I. Helmy, P. Tarafder, and W. Choi, "LSTM-GRU model-based channel prediction for one-bit massive MIMO system," *IEEE Trans. Veh. Tech.*, vol. 72, no. 8, pp. 11 053–11 057, 2023.
- [30] C. Zhang, Y. Jing, Y. Huang, and L. Yang, "Performance analysis for massive MIMO downlink with low complexity approximate zero-forcing precoding," *IEEE Trans. Commun.*, vol. 66, no. 9, pp. 3848–3864, 2018.
- [31] S. S. Christensen, R. Agarwal, E. De Carvalho, and J. M. Cioffi, "Weighted sum-rate maximization using weighted MMSE for MIMO-BC beamforming design," *IEEE Trans. Wireless Commun.*, vol. 7, no. 12, pp. 4792–4799, 2008.
- [32] W. Xia, G. Zheng, Y. Zhu, J. Zhang, J. Wang, and A. P. Petropulu, "A deep learning framework for optimization of MISO downlink beamforming," *IEEE Trans. Commun.*, vol. 68, no. 3, pp. 1866–1880, 2020.
- [33] H. Ye, G. Y. Li, and B.-H. Juang, "Power of deep learning for channel estimation and signal detection in OFDM systems," *IEEE Wireless Commun. Lett.*, vol. 7, no. 1, pp. 114–117, 2018.
- [34] N. Samuel, T. Diskin, and A. Wiesel, "Deep MIMO detection," in *Proc. 18th IEEE Int. Workshop Signal Process. Advances Wireless Commun (SPAWC)*, Hokkaido, Japan, Jul. 2017, pp. 1–5.